particularly in the hills. It may be concluded that high-resolution images need to be orthorectified before processing. Since planimetric accuracy is significant, orthorectification helps to fit the image and outputs in a base map. The quality of orthorectification depends upon the quality of DEM. Therefore, high-resolution DEM needs to be used wherever possible. It is suggested that the loss of information in stretched areas could be supplemented with ground truth.

1. Jensen, J. R., *Introductory Digital Image Processing*, Prentice Hall, New York, 1996, 2nd edn, pp. 24–137.
2. Lillesand, T. M. and Kiefer, R. W., *Remote Sensing and Image Interpretation*, John Wiley, New York, 1999, 4th edn, pp. 5–189.
3. Toutin, T., Geometric processing of remote sensing images. *Int. J. Remote Sensing*, 2004, **25**, 1893–1924.
4. Bannari, A., Morin, D., Benie, G. B. and Bonn, F. J., A theoretical review of different mathematical models of geometric corrections applied to remote sensing images. *Remote Sensing Rev.*, 1995, **13**, 27–47.
5. Tau, C. V. and Hu, Y., Use of rational function model for image rectification. *Can. J. Remote Sensing*, 2001, **27**, 593–602.
6. Dowmann, I. and Dolloff, J. T., An evaluation of rational functions for photogrammetry restitution. *Int. Arch. Photogramm. Remote Sensing*, 2000, **33**, 252–266.
7. Fraser, C. S., Hanley, H. B. and Yamakawa, T., Sub-meter geopositioning with IKONOS geo imagery. In Proceedings of a Joint ISPRS Workshop on High Resolution Mapping from Space 2001, Hannover, Germany, 19–21 September 2001.
8. Cheng, K. S., Yeh, H. C. and Tsai, C. H., An anisotropic spatial modeling approach for remote sensing image rectification. *Remote Sensing Environ.*, 2000, **73**, 46–54.
9. Morad, M., Chalmers, A. I. and O'Regan, P. R., The role of root mean square error in the geo-transformation of images in GIS. *Int. J. Geogr. Inf. Syst.*, 1996, **3**, 347–353.
10. Hinton, J. C., GIS and remote sensing integration for environmental application. *Int. J. Geogr. Inf. Syst.*, 1996, **10**, 877–890.
11. Rocchini, D. and Rita, Di, A., Relief effects on aerial photos geometric correction. *Appl. Geogr.*, 2005, **25**, 159–168.
12. Vassilopoulou, S., Hurni, L., Dietrich, V., Baltsavias, E., Pateraki, M., Lagios, E. and Parcharisdis, I., Orthophoto generation using IKONOS imagery and high-resolution DEM: a case study on volcanic hazard monitoring of Nisyros Island (Greece). *ISPRS J. Photogramm. Remote Sensing*, 2002, **57**, 24–38.
13. Shaker, A., Shi, W. and Barakat, H., Assessment of the rectification accuracy of IKONOS imagery based on two-dimensional models. *Int. J. Remote Sensing*, 2005, **26**, 719–731.
14. Yang, X., Accuracy of rational function approximation in photogrammetry. In Proceedings of ASPRS Annual Convention, American Society of Photogrammetry and Remote Sensing, Washington DC, 22–26 May 2000.
15. Tau, C. V. and Hu, Y., A comprehensive study of the rational function model for photogrammetry processing. *Photogramm. Eng. Remote Sensing*, 2001, **67**, 1347–1357.
16. Mercer, J. B., Allan, J., Glass, N., Rasmussan, J. and Wollersheim, M., http://www.intermap.com/uploads/1170362785.pdf
17. Aguilar, M. A., Aguilar, F. J. and Sanchez, J. A., Geometric accuracy assessment of QuickBird basic imagery using different operational approaches. *Photogramm. Eng. Remote Sensing*, 2007, **12**, 1321–1332.
18. Srivastava, P. K., Krishna, G. B. and Majumdar, K. L., Cartography and terrain mapping using IRS-1C data. *Curr. Sci.*, 1996, **70**, 562–567.
19. Jayaprasad, P., Narendra, B., Arya, A. S. and Ajai, Extraction of terrain parameters from IRS-1C PAN stereo data using photogrammetric techniques. *Curr. Sci.*, 1996, **82**, 562–567.
20. Nagasubramanian, V., Radhadevi, P. V., Ramachandran, R. and Krishna, R., Rational function model for sensor orientation of IRS-P6 LISS IV imagery. *Photogramm. Rec.*, 2007, **22**, 309–320.
21. Konency, G., Methods and possibilities for digital differential rectification. *Photogramm. Eng. Remote Sensing*, 1979, **6**, 727–734.
22. http://www.geoimage.com.au/geoweb/pdfs/products/SRTM_DEMs.pdf
23. www.glcf.umiacs.umd.edu/data/guide/technical/technique_geocover.pdf

ACKNOWLEDGEMENTS. We thank the Department of Biotechnology, New Delhi for funds. We are grateful to Mrs Shefali Agrawal, Poonam Tiwari and Hina Pandey, IIRS, Dehradun for fruitful discussions. We also thank Dr V. K. Dadhwal, IIRS, Dehradun for facilities and encouragement.

Received 5 March 2008; revised accepted 24 September 2008

Estimates of geothermal gradients from bottom simulating reflectors

N. Aravind Kumar, B. Ashalatha, Babita Sinha and N. K. Thakur*

National Geophysical Research Institute, Uppal Road, Hyderabad 500 007, India

Multi-channel seismic reflection data from two different tectonic regimes over the continental margins of India have been studied to identify the bottom simulating reflector (BSR), a prime indicator for the presence of gas hydrates in a region. The probable depth of occurrence of these BSRs is estimated. The estimated depths were projected on plots of hydrate stability zones calculated for different geothermal gradients. The projected depths show scatter over curves of geothermal gradients. Best-fit curves were obtained from the datasets to arrive at geothermal gradients over the two regions. The estimated geothermal gradient for Kerala–Konkan is of the order of 0.05°–0.055°C/m and for Andaman region it is in the range 0.015°–0.02°C/m. The estimated geothermal gradient over Kerala–Konkan indicates normal value, whereas for the tectonically active Andaman region, it is lower. Utilizing the published values of thermal conductivities for hydrated sediments we have determined the heat flow values. The estimated heat flow value for Kerala–Konkan region seems to be normal with hydrated sediments, whereas the value obtained for the Andaman region seems to be significantly low. Possible explanation for this anomalous behaviour has been attempted.

*For correspondence. (e-mail: nkthakur46@yahoo.com)

Keywords: Gas hydrates, geothermal gradient, tectonics, thermal conductivity.

IDENTIFICATION of bottom simulating reflectors (BSRs), on multi-channel seismic reflection data suggests the possible presence of gas hydrates in a region, and depth of their occurrence commonly marks the hydrate phase boundary[1]. The BSR in general is caused by the impedance created by sediments saturated with high-velocity hydrates overlying free gas or brine-saturated sediment with low seismic velocity. The amplitude of the BSR is dependent on the hydrate concentration and porosity of the sediment, and the frequency of the seismic source. BSRs are clearly identified when there is the greatest incoherent deformation, i.e. where the bedding reflectors are the least clear or absent[2]. A second significant seismic characteristic of gas hydrates is the reduction of reflection strength within the gas hydrate zone, a feature called 'blanking'. Blanking apparently is caused either by cementation of the sediment grains by hydrates or due to homogenization within the sediments[3–6].

Hydrate occurs in a relatively shallow, narrow zone termed as the hydrate stability zone (HSZ), which lies almost parallel to the terrestrial surface in permafrost regions or to the seafloor in the oceans. The variables affecting hydrate thickness are ocean bottom depth, temperature, availability of gas (CH_4), hydrate velocity, geothermal gradient, thermal conductivity, heat flow, gas composition, total organic content (TOC) and connate water salinity[7]. Heat flow measurements have been used to lay constraints on the limits of the HSZ zone[8,9]. In regions where geothermal measurements are not available, geothermal gradients and heat flow values can be estimated from the BSR depths[10–12].

Parallelism of a reflector to the seafloor in the HSZ is a prime criterion for identifying BSRs and thereby infers the presence of gas hydrates. In an area where the ocean bottom is smooth, heat flow is generally constant. The measured heat flow in a region is the product of geothermal gradient and thermal conductivity. Thus for constant heat flow, any changes in the thermal conductivity result in a change in the geothermal gradient. Thermal conductivity in the rocks is basically governed by the lithology. In case of sand–shale, the thermal conductivity increases with increase in sand–shale ratio, and the geothermal gradient decreases[7]. Even if the ocean bottom is smooth and flat, the base of the HSZ will not follow the isotherms due to tectonic disturbances. The positions of the isotherms are strongly affected by changes in thermal conductivity associated with different diapiric structures (shale and salt), buried sediment, deep-rooted faults and recent volcanic activity. In relevance of the above, the HSZ pattern is affected by local heat-flow variation associated with different lithology/geology and tectonic processes. Therefore, lateral and vertical changes in the sediment type would affect the depth to the base of the hydrates[7,13,14].

In this communication we study two different tectonic regimes (Figure 1) and estimate the local geothermal gradients and heat flow over the continental margins of India.

The Kerala–Konkan offshore basin on the western continental margin of India evolved during northward motion of the Indian Ocean plate[15]. The initial phase of the rifting formed a system of NNW–SSE horsts and grabens over the western continental margin[16]. The margin is characterized by several basement highs and volcanic intrusive features such as the Chagos–Laccadive volcanic ridge, the Laxmi ridge, the Kori–Comorin depression and ridge, and the Pratap ridge[14].

The Andaman region is tectonically different from the eastern margin of India. The Andaman Sea lies along the Indian and Chinese (Eurasian) plate boundary, which extends from the Sunda Arc and Trench off Java and Sumatra, along the west side of the Andaman–Nicobar ridge and northward through the Indo-Burmese ranges (Figure 2). The Andaman and Nicobar Island group consists of Cretaceous ophiolites with radiolarian cherts, pelagic limestone and quartzite of unknown origin. A thick section of the Eocene and Oligocene Andaman flysch is overlain by Neogene shallow-water sediments of the ridge top and island. The boundary between the Andaman–Nicobar ridge and the Andaman Sea basin is a complex of north-south-trending faults, dividing the sea floor into a series of ridges. The most prominent of these faults is the West Andaman Fault, which is marked by a west-dipping cuesta of sedimentary rocks. All faults shown in Figure 2 are inactive, except the central section[17] where focal mechanism studies indicate a north–south right-lateral motion.

We have estimated the thickness of the HSZ from simultaneous solutions of pressure–temperature equations for the gas hydrate stability phase[18,19]. Information about the ocean bottom temperature has been taken from the International Indian Ocean Expedition atlas. To estimate the effect of geothermal gradient on base of the HSZ, we

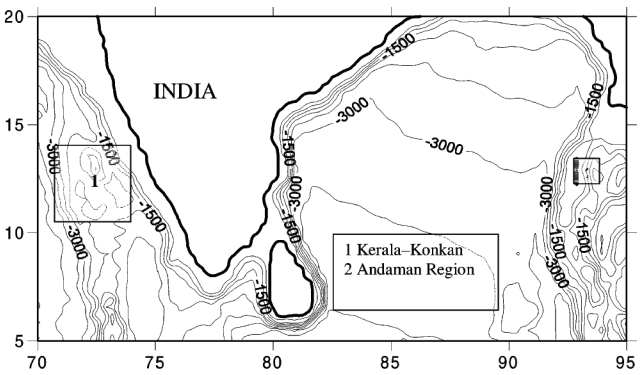

Figure 1. Two different tectonic regimes over which BSRs were identified in the continental margins of India, selected for the present study. Bathymetry contours are also presented.

have generated stability curves for varying water depths (hydrostatic pressure), greater than 1000 m and for different geothermal gradients. A family of curves was obtained by plotting the depth to the base of the HSZ (assuming pure methane hydrate) against the water depth for the Kerala–Konkan and Andaman offshore areas. Each curve assumes a different geothermal gradient.

We have utilized the available information on depth to the BSR and sea floor and determined the local geothermal gradient. In the case of Kerala–Konkan, the two way-travel times (TWT) of BSRs have been converted to depths (m) using an average *P*-wave velocity of 1.8 km/s, which has been determined from multi-channel seismic (MCS) velocity analyses. In the Andaman area the observed BSRs are relatively deep. We have converted the BSR time to depth using two different velocities, i.e. 1.6 and 1.8 km/s, to examine the influence of velocity on the occurrence of the BSR. The observed sets of BSR depths have been plotted on the stability curves generated for different geothermal gradients (Figures 3 and 4). The BSR depth shows scatter and in this regard we have determined a least square fit line to ascertain the representative pattern of BSR variations with depth in two regions. The correspondence of the fitted BSR line with a stability curve derived from one of the geothermal gradients is utilized to arrive at the representative geothermal gradient in these regions.

Heat-flow measurements have facilitated the development of lithospheric models of the ocean basins and marginal seas and indirectly contribute towards the understanding of continental sedimentary basins. The magnitude of the heat flow at a given location depends on: (i) the process of sedimentation and deposition, (ii) sediment compaction, and (iii) presence of gas hydrates. These factors are directly related to thermal conductivity of the sediments and geothermal gradients of a given area. The pattern of thermal conductivity is influenced and inversely related to porosity of the medium under consideration. The porosity of the sediments considerably decreases with weight of the overburden (depth). In this regard the older marine sediments the local thermal conductivity generally increases due to compaction of the sediments (~1–3 $Wm^{-1} K^{-1}$)[20], and to a small extent increases with increasing water depth[21]. For a constant heat flow, a higher thermal conductivity produces lower geothermal gradients, and changes in thermal conductivity due to lateral changes in sediment character may give rise to a localized anomaly in heat flow[8].

In the Kerala–Konkan region we have estimated the geothermal gradients in the range between 0.050° and 0.055°C/m (Figure 3). These values are about 30% higher

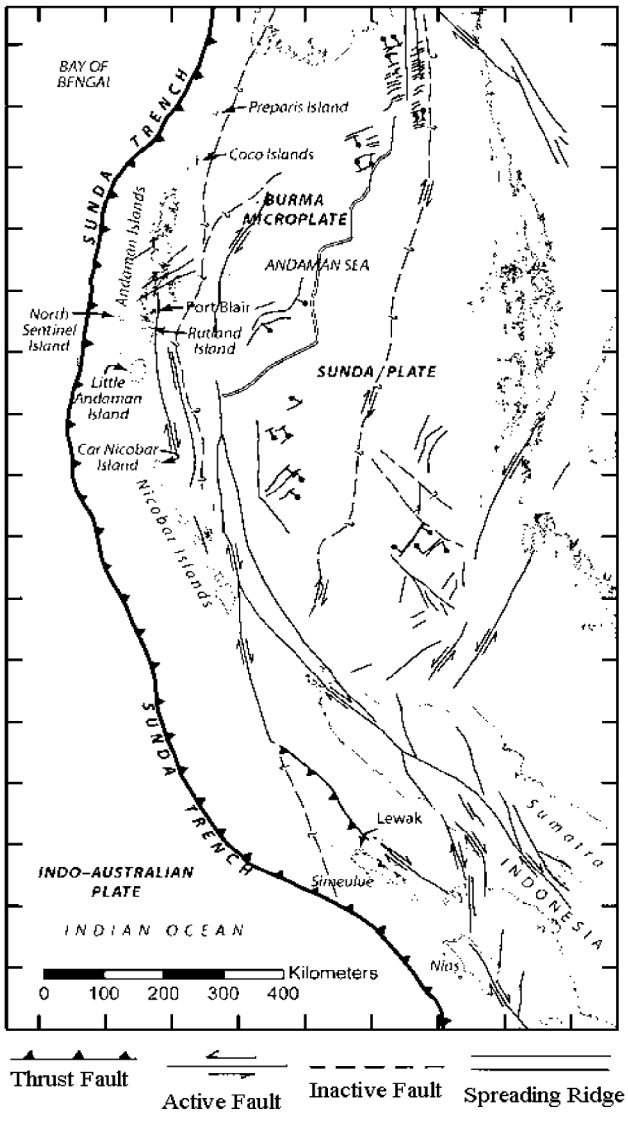

Figure 2. Tectonic map of Burma and the Andaman Sea (after Moore *et al.*[23]).

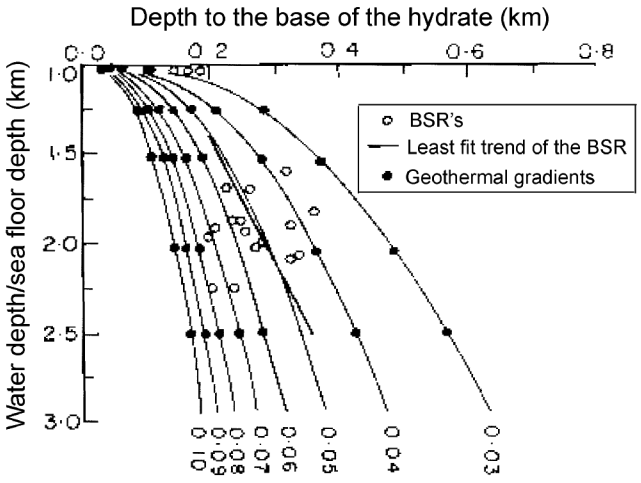

Figure 3. Hydrate stability curves for pure methane hydrate in the Kerala–Konkan region for different geothermal gradients. TWT of BSRs are converted to depths (m) using an average *P*-wave velocity of 1.8 km/s. Solid straight line is the least square best fit for the observed BSR in the region with standard deviation of 0.9×10^{-3}.

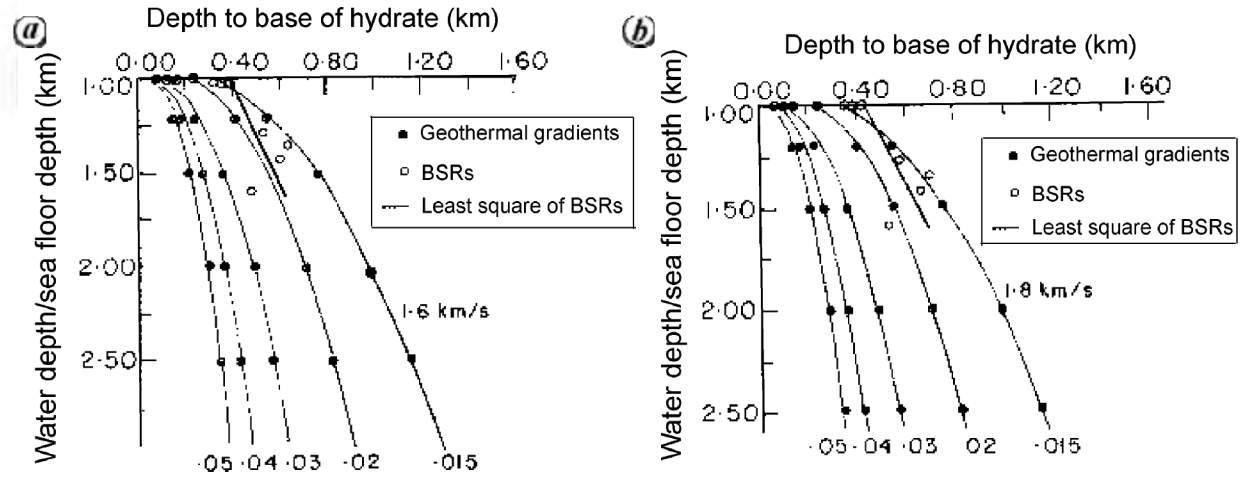

Figure 4. Hydrate stability curves for pure methane hydrate for different geothermal gradients in the Andaman offshore region. TWT of BSRs are converted to depths (m) using two different *P*-wave velocities of (***a***) 1.6 km/s and (***b***) 1.8 km/s. The solid straight line is the least square best fit for observed BSR in the region with standard deviation of 0.7×10^{-3} for (***a***) and 0.9×10^{-3} for (***b***).

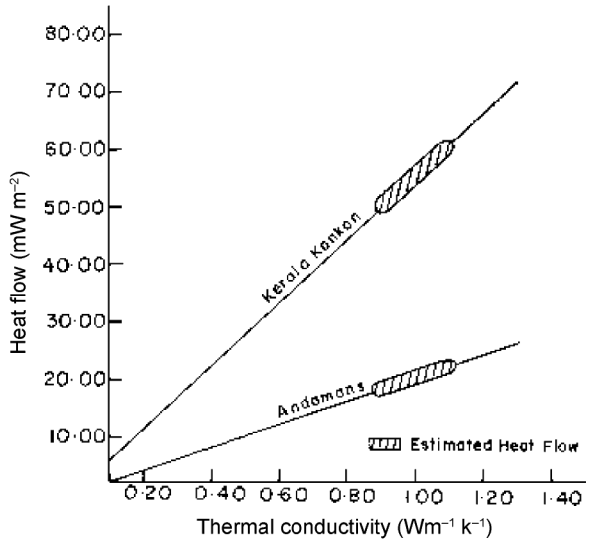

Figure 5. Estimated heat flow range in the Kerala–Konkan and Andaman areas. Geothermal gradients of 0.055° and 0.020°C/m were utilized for gas hydrate saturated sediments in Kerala–Konkan and Andaman areas respectively.

than that obtained earlier[12]. This discrepancy may be due to different methods used. We have determined the geothermal gradient which fits best for all the BSRs observed in this area, whereas the earlier studies utilized data from one BSR identified on a seismic line. It has been suggested[21] that in deep-ocean sediments, the geothermal gradient is of the order of 0.038–0.058°C/m. It has also been established[22] that the thermal conductivity of pure hydrate is about 30% less than that of water. If the water in the sediment is replaced by 10–20% hydrates, a decrease of about 23% in the overall thermal conductivity is observed (a decrease of 40% in the case of sand, if the pores are saturated with propane hydrate).

To get an estimate of heat flow we have considered thermal conductivities in the range 0.9–1.1 $Wm^{-1} K^{-1}$, representative of sediment grains cemented with gas hydrates. Considering the estimated value of 0.055°C/m as the geothermal gradient for the Kerala–Konkan region, the obtained heat-flow value ranges from 50 to 60 mW m^{-2} (Figure 5). We have considered lower thermal conductivity in comparison to earlier studies in relevance to what was been discussed above.

The decrease in thermal conductivity would result in a slight increase in the geothermal gradient in order to keep the heat flow constant. Under these circumstances, the estimated geothermal gradient over the Kerala–Konkan region seems to be normal.

The obtained geothermal gradient (0.012°–0.018°C/m) for the Andaman region agrees well with that reported earlier[23]. Moore *et al.*[24] have reported heat-flow values of the order of 3.3–5.9 heat flow units, which corresponds to 140–240 mW m^{-2}. Such high heat-flow values have been obtained considering normal thermal conductivities of the oceanic sediments. If these sediments are saturated with gas hydrates, their presence tends to reduce the thermal conductivity and thereby the geothermal gradient in this region. Considering the determined geothermal gradient of 0.012–0.018 and assuming the thermal conductivity of gas hydrate-bearing sediments (0.9–1.1 $Wm^{-1} K^{-1}$), the estimated heat flow would be 15–20 mW m^{-2}, which is significantly low compared to those estimated by earlier studies. The occurrence of deeper BSRs in the Andaman region suggests that the geothermal gradient in this region should be much lower compared to the Kerala–Konkan basin, and the present analysis confirms such observations. The discrepancy between the estimated heat flow in the present study and that observed by earlier studies has be resolved by making heat-flow measure-

ments, to assess the contribution from the age of the lithosphere and due to saturation of sediments by gas hydrates.

Seismic data from two potential gas hydrate-bearing zones with different tectonic regimes have been analysed to arrive at the probable geothermal gradient and heat flow values. Over the Kerala–Konkan region the estimated geothermal gradient is in the range 0.050–0.055°C/m, which seems to be within normal limits. Over the Andaman region the estimated geothermal gradient ranges from 0.015° to 0.020°C/m, which is low for the tectonically active back-arc region.

The low geothermal gradient over the Andaman area has been earlier attributed to the age of the lithosphere in this region, with normal thermal conductivities values of deep ocean sediments, without taking into consideration the effect of thermal conductivity of gas hydrate-bearing sediments.

The heat-flow values over the Kerala–Konkan and Andaman regions have been estimated using the thermal conductivity of sediments saturated with gas hydrates and obtained representative values for geothermal gradients. The estimated heat-flow value for the Kerala–Konkan region is normal, whereas that obtained for the Andaman region is low.

In context of the above, the present study proposes the measurement of heat-flow values in both the regions to signify the contribution from the gas-hydrate bearing layer to the observed heat-flow values.

1. Shipley, T. H., Houston, M., Buffler, R. T., Shaub, F. J., McMillan, K. J., Ladd, J. W. and Worzel, J. L., Seismic reflection evidence for the widespread occurrence of possible gas-hydrate horizons on continental slopes and rises. *AAPG Bull.*, 1979, **63**, 2204–2213.
2. Chapman, N. R., Gettrust, J. F., Walia, R., Hannay, D., Spence, G. D., Wood, W. T. and Hyndman, R. D., High-resolution, deep-towed, multi-channel seismic survey of deep-sea gas hydrates off western Canada. *Geophysics*, 2002, **67**, 1038–1047.
3. Lee, M. W., Hutchinson, D. R., Dillon, W. P., Miller, J. J., Agena, W. F. and Swift, B. A., Method of estimating the amount of *in situ* gas hydrates in deep marine sediments. *Mar. Pet. Geol.*, 1993, **10**, 493–506.
4. Holbrook, W. S., Hoskins, H., Wood, W. T., Stephen, R. A. and Lizarralde, D., Leg 164 Scientific Party, methane hydrate and free gas on the Blake ridge from vertical seismic profiling. *Science*, 1996, **273**, 1840–1843.
5. Wood, W. T. and Ruppel, C., Seismic investigations of the Blake ridge gas hydrate area: a synthesis proceedings of the Ocean drilling program. In ODP Scientific Results (eds Paull, C. K. *et al.*), 2000, vol. 164, pp. 253–264.
6. Holbrook, W. S., Seismic studies of the Blake ridge: implications for gas hydrate distribution, and free gas dynamic. In *Natural Gas Hydrates: Occurrence, Distribution and Detection* (eds Paull, C. K. and Dillon, W. P.), Geophysical Monograph, American Geophysical Union, 2001, vol. 124, pp. 235–256.
7. Macleod, M. K., Gas hydrates in ocean bottom sediments. *AAPG Bull.*, 1982, **66**, 2649–2662.
8. Hutchison, I., Louden, K. E., White, R. S. and Vontterzen, R. P., Heat flow and age of the Gulf of Oman. *Earth Planet. Sci. Lett.*, 1981, **56**, 252–262.
9. Delisle, G., Beiersdorf, N. S. and Steinmann, D., The geothermal field of the North Sulawesi accretionary wedge and a model on BSR migration in unstable depositional environments. In *Gas Hydrates: Relevance to World Marine Stability and Climate Change* (eds Henriet, J. P. and Mienert, J.), Geological Society, London, Special Publication, 1998, vol. 137, pp. 267–274.
10. Davis, E. E., Hyndman, R. D. and Villinger, H., Rates of fluid expulsion across the northern Cascadia accretionary prism: constraints from new heat flow and multi-channel seismic reflection data. *J. Geophys. Res.*, 1990, **95**, 8869–8889.
11. Yamno, M., Uyeda, S., Aoki, Y. and Shipley, T. H., Estimates of heat flow derived from gas hydrates. *Geology*, 1982, **10**, 339–343.
12. Uma Shankar, Thakur, N. K. and Reddi, S. I., Estimation of geothermal gradient and heat flow from Bottom Simulating Reflector along Kerala–Konkan basin of Western Continental Margin of India. *Curr. Sci.*, 2004, **87**, 250–253.
13. Petersen, K. and Lerche, I., Quantitative modeling of salt and sediment interactions: Evolution of a North Louisiana salt diapir. *J. Petrol. Geol.*, 1995, **18**, 365–396.
14. Dillon, W. P. and Max, M. D., Oceanic gas hydrates. In *Natural Gas Hydrates in Oceanic and Permafrost Environments* (ed. Max, M. D.), Kluwer, London, 2003, pp. 61–76.
15. Naini, B. R. and Talwani, M., Structural framework and the evolutionary history of the continental margin of western India. *AAPG Mem.*, 1982, **34**, 167–191.
16. Biswas, S. K. and Singh, N. K., Western India deep-sea basin, Exploration thrust area. *Bull. Oil Nat. Gas Comm.*, 1991, **25**.
17. Curray, J. R., Emmel, F. J., Moore, D. G. and Raitt, R. W., Structure, tectonics and geological history of the northeastern Indian Ocean. In *The Ocean Basins and Margins, Vol. 6, The Indian Ocean* (eds Nairn, A. E. M. and Stehli, F. G.), Plenum Press, New York, 1982, pp. 399–450.
18. Miles, P. R., Potential distribution of methane hydrate beneath the European continental margins. *Geophys. Res. Lett.*, 1995, **22**, 3179–3182.
19. Hanumantha, R. Y., Subrahmanyam, C., Sharma, S. R., Rastogi, A. A. and Deka, B., Estimates of geothermal gradients and heat flow from BSRs along the western margin of India. *Geophys. Res. Lett.*, 2001, **28**, 355–358.
20. Lister, C. R. B., Sclater, J. G., Davis, E. E., Villinger, H. and Nagihara, S., Heat flow maintained in ocean basins of great age: investigations in the north-equatorial West Pacific. *Geophys. J. Int.*, 1990, **102**, 603–628.
21. Langseth Jr, M. G. and Von Herzen, R. P., Heat flow through the floor of world oceans. In *The Sea* (ed. Maxwell, A. E.), 1970, vol. 4, pp. 299–348.
22. Stoll, R. D. and Bryan, G. M., Physical properties of sediments containing gas hydrate. *J. Geophys. Res.*, 1979, **84**, 1629–1634.
23. Max, M. D., Gas hydrate potential of the Indian sector of the NE Arabian Sea and northern Indian Ocean. In *Natural Gas Hydrates in Oceanic and Permafrost Environments*, Kluwer, 2003, pp. 213–224.
24. Moore, G. F., Curray, J. R., Moore, D. G. and Karig, D. E., Variations in geologic structures along the Sunda fore-arc, northeastern Indian Ocean. In *The Tectonic and Geologic Evolution of Southeast Asian Seas and Island* (ed. Hayes, D. E.), American Geophysical Union Monograph, 1980, vol. 23, pp. 145–160.

ACKNOWLEDGEMENTS. We thank the Director, National Geophysical Research Institute, Hyderabad for permission to publish this paper. N.K.T. thanks to CSIR, New Delhi for the Emeritus Scientist position.

Received 19 September 2007; revised accepted 10 September 2008